The photochemical reactions of DNA 6-TG have implications for skin cancer. In a clinical setting, DNA 6-TG and UVA are likely to interact in the skin of organ transplant patients. Around 25,000 solid organ transplants are performed annually throughout Europe and in North America. SCC is 50 to 250 times more common among transplant patients than in the general population (*21*, *22*), and 20 years after transplant, between 60 and 90% of patients are affected (*23*). Transplant-related SCC develops primarily on chronically sun-exposed skin, and sunlight plus the duration of treatment with immunosuppressive drugs are acknowledged risk factors. Until recently, most transplant patients have been treated with Aza. UVA is the major component of solar radiation, and a high fraction of incident UVA penetrates to the basal layers of the skin containing the stem cells. To date, epidemiological studies have not identified the contributions of individual immunosuppressive agents to transplant-related SCC (*23*, *24*). The photochemical properties of DNA 6-TG described here indicate how UVA and an immunosuppressive drug might contribute to post-transplant SCC: a significant cause of morbidity in this group of patients.

References and Notes

1. M. V. Relling, T. Dervieux, *Nat. Rev. Cancer* **1**, 99 (2001).
2. V. J. Hemmens, D. E. Moore, *Photochem. Photobiol.* **43**, 247 (1986).
3. J. Cadet, T. Douki, D. Gasparutto, J.-L. Ravanat, *Mutat. Res.* **531**, 5 (2003).
4. D. E. Barnes, T. Lindahl, *Annu. Rev. Genet.* **38**, 445 (2004).
5. P. Karran, *Carcinogenesis* **22**, 1931 (2001).
6. C. M. H. Driscoll *et al.*, *Solar Radiation Measurements at the Network of Six Sites in the UK, January-December 2001* (National Radiological Protection Board, Oxford, UK, 2002).
7. P. Branch, M. Masson, G. Aquilina, M. Bignami, P. Karran, *Oncogene* **19**, 3138 (2000).
8. E. A. Drobetsky, J. Turcotte, A. Chateauneuf, *Proc. Natl. Acad. Sci. U.S.A.* **92**, 2350 (1995).
9. I. L. Doerr, I. Wempen, D. A. Clarke, J. J. Fox, *J. Org. Chem.* **26**, 3401 (1961).
10. H.-R. Rackwitz, K.-H. Scheit, *Chem. Ber.* **107**, 2284 (1974).
11. J. M. Finkel, *J. Pharm. Sci.* **64**, 121 (1975).
12. H. P. Rappaport, *Biochemistry* **32**, 3047 (1993).
13. A. R. Lehmann, *Mutat. Res.* **509**, 23 (2002).
14. C. Masutani *et al.*, *Nature* **399**, 700 (1999).
15. P. Gruz *et al.*, *J. Biol. Chem.* **276**, 47394 (2001).
16. D. J. Warren, A. Andersen, L. Slordal, *Cancer Res.* **55**, 1670 (1995).
17. C. Cuffari, D. Y. Li, J. Mahoney, J. Y. Barnes, T. M. Bayless, *Dig. Dis. Sci.* **49**, 133 (2004).
18. R. J. Berg, H. J. Ruven, A. T. Sands, F. R. deGruijl, L. H. Mullenders, *J. Invest. Dermatol.* **110**, 405 (1998).
19. A. R. Young, J. M. Sheehan, C. A. Chadwick, C. S. Potten, *J. Invest. Dermatol.* **115**, 37 (2000).
20. N. Al-Tassan *et al.*, *Nat. Genet.* **30**, 227 (2002).
21. B. Lindelof, B. Sigurgeirsson, H. Gabel, R. S. Stern, *Br. J. Dermatol.* **143**, 513 (2000).
22. S. Euvrard, J. Kanitakis, A. Claudy, *N. Engl. J. Med.* **348**, 1681 (2003).
23. H. M. Ramsay, A. A. Fryer, C. M. Hawley, A. G. Smith, P. N. Harden, *Br. J. Dermatol.* **147**, 950 (2002).
24. M. T. Glover, J. J. Deeks, M. J. Raftery, J. Cunningham, I. M. Leigh, *Lancet* **349**, 398 (1997).
25. A. Massey, Y.-Z. Xu, P. Karran, *Curr. Biol.* **11**, 1142 (2001).
26. G. Phear, W. Armstrong, M. Meuth, *J. Mol. Biol.* **209**, 577 (1989).

27. We thank M. Yamada for her kind gift of the SsoP2Y1 DNA polymerase and the staff of the Oligonucleotide Synthesis Laboratory, Cancer Research UK, for oligonucleotides. The work was supported in part by a Royal Society K. C. Wong Fellowship to X.Z. while on leave from Shanghai Jiao Tong University. We also acknowledge support from the Spanish Ministerio de Educacion y Ciencia (to B.M.) and from the Association for International Cancer Research. All studies involving patients were carried out with prior local ethics committee approval. The procedures involved and their implications were fully explained to the patients who gave informed consent.

Supporting Online Material

www.sciencemag.org/cgi/content/full/309/5742/1871/DC1
Materials and Methods
SOM Text
Figs. S1 to S4
Table S1
References

29 April 2005; accepted 4 August 2005
10.1126/science.1114233

Extensive Diversity of Ig-Superfamily Proteins in the Immune System of Insects

Fiona L. Watson,* Roland Püttmann-Holgado,* Franziska Thomas,† David L. Lamar,‡ Michael Hughes, Masahiro Kondo, Vivienne I. Rebel,§ Dietmar Schmucker‖

The extensive somatic diversification of immune receptors is a hallmark of higher vertebrates. However, whether molecular diversity contributes to immune protection in invertebrates is unknown. We present evidence that *Drosophila* immune-competent cells have the potential to express more than 18,000 isoforms of the immunoglobulin (Ig)-superfamily receptor Down syndrome cell adhesion molecule (Dscam). Secreted protein isoforms of Dscam were detected in the hemolymph, and hemocyte-specific loss of Dscam impaired the efficiency of phagocytic uptake of bacteria, possibly due to reduced bacterial binding. Importantly, the molecular diversity of *Dscam* transcripts generated through a mechanism of alternative splicing is highly conserved across major insect orders, suggesting an unsuspected molecular complexity of the innate immune system of insects.

Immunoglobulin (Ig)-domain-containing proteins constitute the largest repertoire of surface receptors in animals and serve many functions in molecular recognition, cell adhesion, and signaling. Most striking is the exceptional diversity of antigen-specific receptors of the adaptive immune system in higher vertebrates, which depends on somatic gene rearrangement and clonal selection. However, somatic rearrangement of highly diverse immune receptors has been considered to exist in a relatively small number of animal species restricted to the jawed vertebrates (*1*, *2*).

We previously identified a single *Drosophila Dscam* gene as a member of the Ig superfamily and initially characterized its essential function in neuronal wiring (*3*). Gene organization of *Dscam* comprises clusters of variable exons flanked by constant exons (Fig. 1A) (*3*). Although mechanistically entirely different from somatic rearrangements, alternative splicing of the *Dscam* gene combines constant and variable exons by mutually exclusive splicing and potentially generates as many as 19,008 different extracellular domains. Therefore, it is conceivable that a large protein isoform repertoire with the potential for recognizing diverse ligands and epitopes could be generated (*3*). To explore this, we undertook a comparative and functional analysis of *Dscam* expression in immune-competent cells of flies and other insects.

Fat body cells and hemocytes (i.e., insect blood cells) constitute important cells of the insect immune system (*4*–*6*). Most proteins in insect hemolymph, the insect equivalent of blood serum, are produced in fat body cells, which also secrete antimicrobial peptides that constitute an important component of the humoral immune defense (*7*). In contrast, hemocytes are involved in cellular defense strategies such as phagocytosis and wound repair (*8*).

In situ hybridization of tissue from third instar *Drosophila* larvae with a Dscam-specific probe (*9*) revealed Dscam expression in fat

Department of Cancer Biology, Dana Farber Cancer Institute, Department of Neurobiology, Harvard Medical School, Boston, MA 02115, USA.

*These authors contributed equally to this work.
†Present address: Boehringer Ingelheim Pharma KG, 88397 Biberach, Germany.
‡Present address: Department of Medicine, Emory University School of Medicine, Atlanta, GA 30322, USA.
§Present address: Children's Cancer Research Institute, University of Texas Health Science Center, San Antonio, TX 78229, USA.
‖To whom correspondence should be addressed. E-mail: dietmar_schmucker@dfci.harvard.edu

body cells (fig. S1). For a comparison of Dscam expression in immune and neural tissue we isolated mRNA from larval hemocytes, fat body and brain tissue (*9*). Hemocyte-specific green fluorescent protein (GFP) expression allowed for the purification of hemocytes by fluorescence activated cell sorting (FACS) (fig. S3) (*9*). Reverse transcription polymerase chain reaction (RT-PCR) analysis and sequencing of ~50 cDNAs revealed that the majority of Dscam mRNAs in hemocytes, fat body, and brain contain unique exon 4 to 6 combinations (table S1) (*9*).

For a global assessment of alternative splicing in different cell types we used custom-made oligo-arrays (*9*). Microarrays contained specific 50-mer oligo-probes for all alternatively spliced exons. Dscam mRNA sequences were amplified by RT-PCR, and cDNAs were fluorescently labeled and hybridized to the microarrays (*9*) (Fig. 1, B to D). We found that 59 of the 60 alternative exon 4 and exon 6 sequences were expressed in all three cell types. In brain tissue, 32 exon 9 sequences were expressed (Fig. 1D). However, only a subset (total of 14) was expressed in fat body cells and a slightly different subset (total of 15) was expressed in hemocytes (Fig. 1D). On the basis of relative expression amounts, we estimate that 80 to 90% of all Dscam mRNAs in hemocytes and fat body contain exon 9.6, 9.9, 9.13, 9.30, or 9.31, demonstrating that exon 9 splice variants in fat body cells and hemocytes are distinct from those found in brain (Fig. 1D and fig. S2B). Considering all of the alternative exons detected (12 for exon 4, 47 for exon 6, 16 for exon 9, and 2 for exon 17), we calculate that this potentially allows for the generation of more than 18,000 diverse receptor isoforms in fat body cells and hemocytes (Fig. 1) (*9*).

We raised antibodies against extracellular (D-ex1, D-ex2) and intracellular (D-cy) domains of Dscam (Fig. 2A) (*9*). All antibodies recognized an ~210-kD endogenous form of Dscam in extracts from cultured S2 cells (Fig. 2, B to D), a cell line thought to be derived from embryonic hemocytes and shown to share many characteristics with hemocytes (*10*, *11*). A 210-kD form of Dscam was also confirmed in purified larval hemocytes (Fig. 2, C and D, and fig. S3) (*9*), fat body tissue, and at comparatively high amounts in brain (Fig. 2, D and E).

Immunoprecipitations from fat body extracts revealed three Dscam forms (Fig. 2E), possibly representing truncated forms generated by proteolytic cleavage. Unexpectedly, we found that S2 cell-conditioned medium contained a soluble Dscam protein of ~160 kD (Fig. 2F) and that a secreted Dscam protein of the same molecular weight was also present in hemolymph serum (Fig. 2G).

Liquid chromatography and tandem mass spectrometry (LC-MS/MS) directly confirmed that S2 cells secrete Dscam isoforms (*9*) (table S2 and fig. S4). Coverage of the secreted forms by the identified peptides amounts to more than 50% of the entire extracellular part of Dscam (fig. S4A). Importantly, some of the identified peptides confirmed the presence of alternatively spliced sequences, including five Ig2 sequences and at least 12 Ig3 sequences (table S2 and fig. S4, B and C). In agreement with the expression profiling of exon 9 (Ig7) sequences (Fig. 1), we identified three distinct Ig7 domains (i.e., $Ig7^{6}$, $Ig7^{9}$, and $Ig7^{13}$), which correspond to the most abundantly expressed exon 9 sequences (Fig. 1 and fig. S2B).

Considering the protein sequencing results (table S2 and fig. S4), the presence of secreted Dscam in hemolymph (Fig. 2), and the large pool of diverse Dscam mRNAs in fat body cells or hemocytes (Fig. 1D), it is possible that thousands of Dscam isoforms circulate in the hemolymph of *Drosophila*.

We next sought to determine whether Dscam proteins are functionally required in immune-competent cells. However, because animals with homozygous amorphic mutations in *Dscam* die as embryos (*3*, *12*), it was not possible to directly test this in null mutant animals. Nevertheless, we were able to purify GFP-labeled hemocytes from *Dscam* mutant larvae that carry a transallelic combination of hypomorphic ($Dscam^{39}$) and amorphic ($Dscam^{20}$) mutations (*13*). Immunoblotting showed that $Dscam^{20}/Dscam^{39}$ animals have a strong overall reduction in protein concentration (Fig. 3A). One important function of hemocytes is the ingestion of bacterial pathogens by phagocytosis (*8*). We therefore challenged wild-type and Dscam-deficient hemocytes with heat-killed fluorescently labeled *Escherichia coli* and determined the number of hemocytes containing fluorescent bacteria [phagocytic index (Fig. 3B and fig. S5)] (*9*). Normal

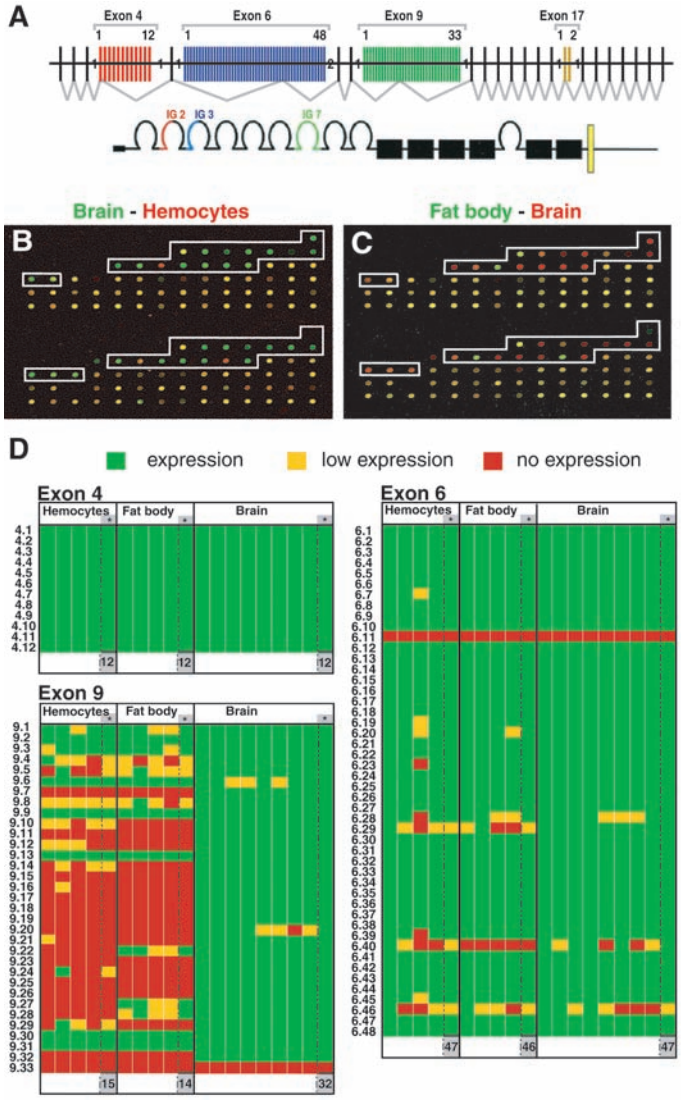

Fig. 1. Dscam isoform expression in hemocytes and fat body tissue. (**A**) Gene and protein structure of *Drosophila* Dscam. Mutually exclusive alternative splicing occurs for exon clusters 4, 6, 9, and 17 (*3*). (**B** and **C**) Alternative exon expressions in brain and hemocytes (B) or brain and fat body cells (C). Microarrays were hybridized with Cy3- and Cy5-labeled cDNA (*9*), and one representative array from slides that contain triplicate arrays is shown. Spots corresponding to exon 9 sequences are indicated by a box (white line) and reveal predominant expression in brain tissue. (**D**) Summary of expression data for all alternative exons. Every exon is represented by a single colored square: moderate to high expression (green), low expression (yellow), and very low or no expression (red). For quantitative evaluation and definition of thresholds, see (*9*). Four experiments for hemocytes or fat body cells and eight for brain tissue were analyzed and presented as adjacent columns. Average values are listed separately in last column (marked by asterisks). Total number of exons expressed is given at bottom. Restricted usage of exon 9 is consistent with expression profiling studies comparing different neuronal cell types (*12*) as well as photoreceptor neurons and S2 cells (*24*).

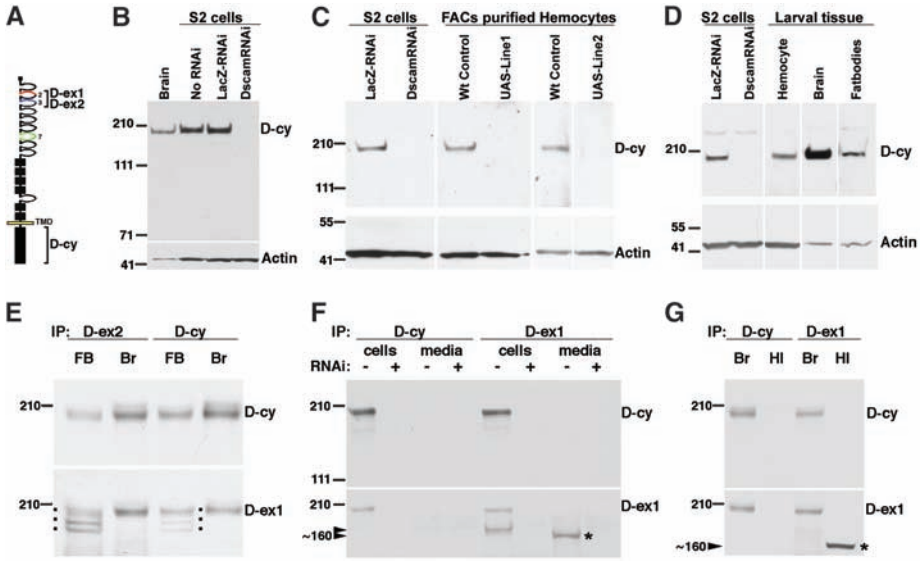

Fig. 2. Dscam protein is expressed in immune-competent cells. (**A**) Proteins recognized by antibodies to Dscam D-cy, D-ex-1, and D-ex-2. (**B**) Dscam protein ~210 kD in S2 cells and in brain tissue (Brain) lysates. RNAi treatment (DscamRNAi) in S2 cells selectively depletes expression of the 210-kD band compared with untreated (no RNAi) or control-treated (LacZ-RNAi) cells. (**C**) Hemocytes isolated from independent transgenic lines (UAS-Line1 and UAS-Line2) of larvae that express dsDscam-RNA(9) (RNAi knock-down) have strongly reduced Dscam protein amounts compared with control (Wt Control, lanes 3 and 5). (**D**) Full-length Dscam protein (~210 kD) is present in fat bodies (three fat bodies per lane), purified hemocytes (3×10^4 cells per lane) (*9*), and brain (one brain per lane). S2 cells (1×10^4 cells per lane) treated with control dsRNA (LacZ-RNAi) or Dscam dsRNA (DscamRNAi) show specificity of Dscam detection. (**E**) Dscam protein was immunoprecipitated (IP) from fat body (FB) or brain (Br) by using D-ex2 or D-cy. Western blot analysis detects 3 Dscam protein forms (•) in fat bodies (*9*). (**F**) Dscam protein IP from lysates of S2 cells (cells) or conditioned media (media) using D-cy (lanes 1 to 4) or D-ex1 (lanes 5 to 8). Western blot analysis using D-cy (top) or D-ex1 (bottom) indicate presence of shorter protein forms in S2 cells (lane 5). The smaller ~170-kD band (top arrowhead) likely represents a Dscam protein lacking a cytoplasmic domain. A truncated Dscam protein of ~160 kD (bottom arrowhead) is only detected in S2 cell-conditioned media lane 7, marked with asterisk). Dscam RNAi–treated samples (+) and LacZ RNAi–treated control samples (–) served as controls. (**G**) Brain tissue (Br) or larval hemolymph (Hl) were immunoprecipitated with D-ex1 or D-cy. Western blot analysis reveals a truncated Dscam protein of ~160-kD in hemolymph (lane 4, marked with asterisk) not detected with D-cy (lane 2).

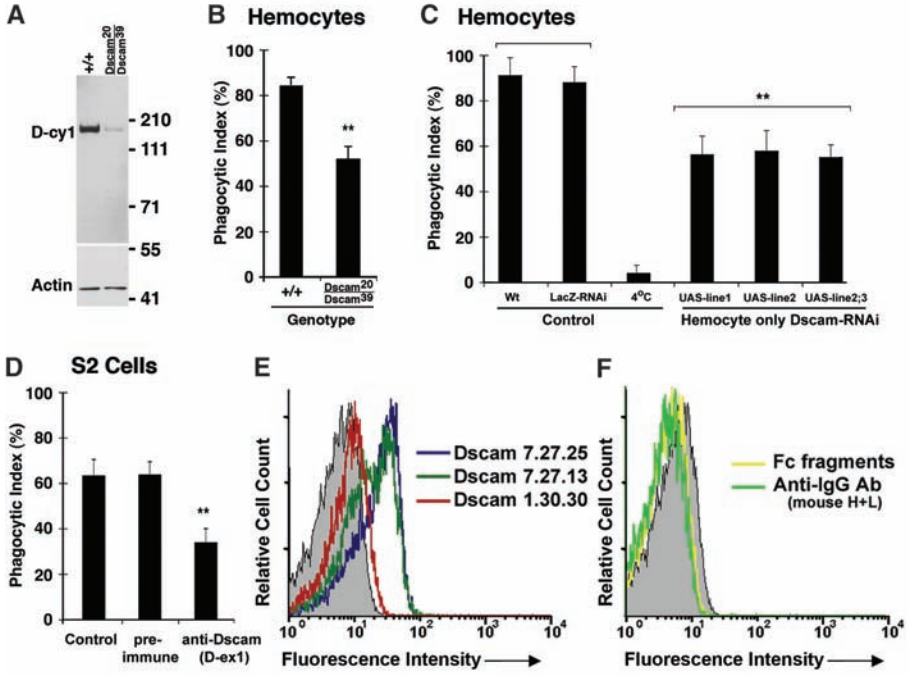

Fig. 3. Dscam is required in hemocytes for efficient phagocytosis and binds to *E. coli*. (**A**) Western blot analysis of larval brain tissue from control (+/+) or $Dscam^{39}/Dscam^{20}$ larvae reveals strong reduction of Dscam protein concentration. (**B**) Phagocytosis assays (*9*) were performed on hemocytes isolated from $Dscam^{39}/Dscam^{20}$ mutant larvae. Significant reduction (marked by double asterisks) in phagocytosis was found in Dscam-deficient hemocytes but not wild-type (+/+) hemocytes. (**C**) Assays performed on Dscam-deficient hemocytes (Dscam-RNAi). Hemocytes from three independent UAS lines showed a significant reduction ($P < 0.01$) compared with wild-type (Wt) or ds-LacZ RNA-treated hemocytes (LacZ-RNAi) (*9*). (**D**) Treatment of S2 cells with neutralizing antibody to Dscam significantly ($P < 0.01$) decreases phagocytosis. S2 cell treatment with either Schneider media vehicle control (control) or the pre-immune serum (pre-immune) served as controls. Error bars in (B) to (D) indicate SEM. (**E** and **F**) Dscam isoforms show binding to *E. coli* bacteria (DH5α strain). Binding of Fc-tagged recombinant proteins (E) or control antibodies (F) was detected by FACS (*9*) using Alexa–Fluor (Molecular Probes, Eugene, OR) 488 conjugated to protein A. (E) Dscam-7.27.25 isoform (blue) and Dscam-7.27.13 isoform (green) show binding when compared with the control sample incubated with protein A Alexa–Fluor 488–conjugated only (gray). Dscam-1.30.30 (red) shows no binding above background. (F) Fc peptides (yellow) and an unrelated mouse antibody (Anti-IgG, green) exhibited no binding and were used as negative controls.

hemocytes exhibited highly efficient phagocytosis, and 85 to 90% had taken up bacteria after 10 min (Fig. 3B). In contrast, only 55% of Dscam mutant cells had taken up bacteria (Fig. 3B).

To investigate more directly the possible role of Dscam in immune defenses, we addressed three questions: First, is Dscam cell autonomously required for phagocytosis in hemocytes? Second, can antibodies that specifically bind extracellular Ig domains of Dscam acutely interfere with phagocytosis? Third, can Dscam isoforms directly bind to pathogens?

We used expression of double-stranded RNA [i.e., RNA interference (RNAi)] to suppress Dscam expression in transgenic flies (*9*) (Fig. 3C). A *hemolectin* promoter region–GAL4 fusion, termed Hml-GAL4, was used for activating expression exclusively in embryonic and larval hemocytes (*14*, *15*). Hemocytes with Dscam-specific knock-down showed a substantially reduced rate of phagocytosis, with less than 60% of the cells containing bacteria (Fig. 3C). This partial inhibition may reflect RNAi-mediated knock-down in only a subset of the highly heterogeneous cell population of larval hemocytes (*8*, *16*). We therefore examined S2 cells, which represent a less heterogeneous cell population also capable of phagocytosis (Fig. 3D), and used antibodies to Dscam to block Dscam function (*9*). We reasoned that the short application of antibodies against Dscam, in contrast to continuous RNAi, may be less likely to influence general hemocyte characteristics or development (*8*, *16*). Treatment of S2 cells with polyclonal α-Dscam serum D-ex1 resulted in a 30% decrease in the phagocytic index (Fig. 3D). It is possible that the α-Dscam antibody

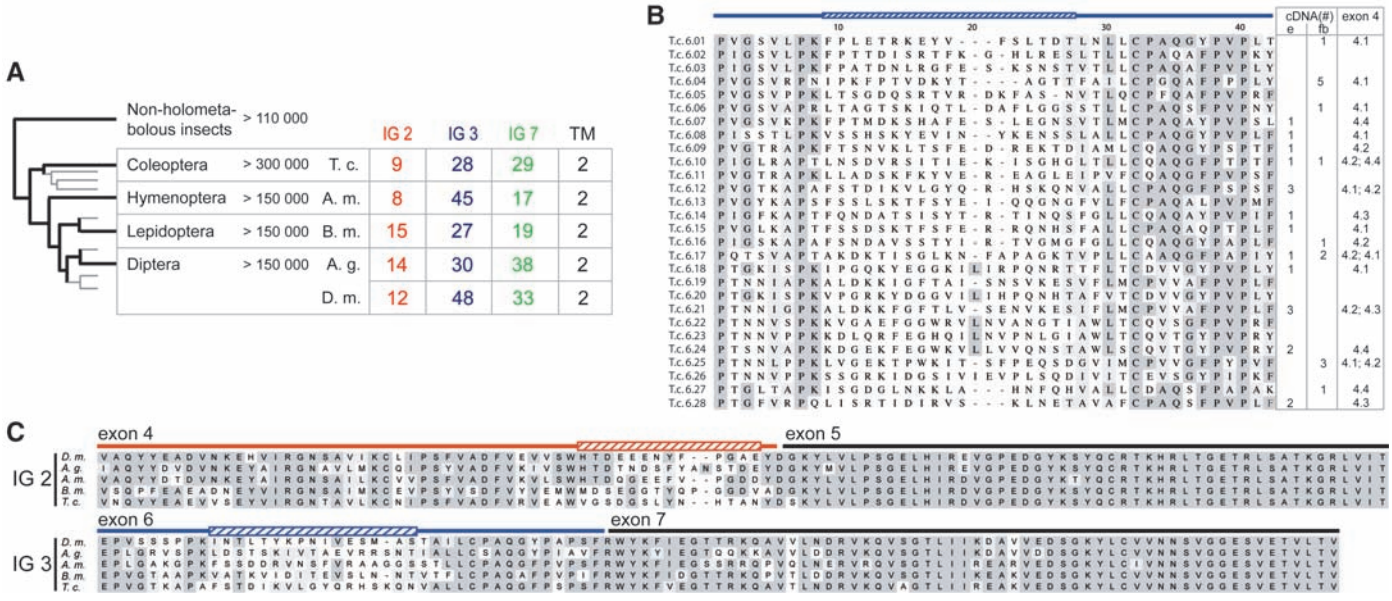

Fig. 4. Conservation of Dscam diversity in insects. (**A**) Simplified phylogenetic tree indicating estimated number of species. Orders with less than 7000 species are indicated by gray lines (*18*). Alternative splicing is present in all holometabolous insect orders. Abbreviations are as follows: *T. castaneum*, T.c.; *Apis mellifera*, A.m.; *Bombyx mori*, B.m.; *Anopheles gambiae*, A.g.; and *D. melanogaster*, D.m. Table lists number of exons identified. (**B**) Alignment (*25*)of Ig3 sequences (N-terminal half) of *Tribolium*. Twenty-eight alternative exons are predicted to encode Ig3 sequences or verified by RT-PCR from embryonic (e) or fat body (fb) tissues (*9*). Numbers of cDNAs are listed on right side. Gray shading indicates conserved amino acids. (**C**) Sequence alignment of the Ig domains 2 and 3 of *D. melanogaster*, *Anopheles gambiae*, *B. mori*, *Apis mellifera*, and *T. casteneum*. Despite the large evolutionary distances, C-terminal halves of Ig2 and Ig3 are nearly identical. A highly conserved Ig-domain scaffold embeds alternatively spliced sequences, which are species-specific and show little conservation. Variable N-terminal half of Ig2 and Ig3 reveal distinct high variability regions (hatched rectangles). Location of variability hot spots is conserved across species. Note that the locations of sequence variability in Dscam Ig domains is distinctly different from variability in complementary determining regions of V-type Ig domains of mammalian immune receptors. Ig2 domains are most variable at the end of exon 4, likely to correspond to the C′ strand of the Ig-fold. Ig3 domains are most variable at the middle of exon 6, possibly corresponding to the A and A′ strands, similar to *Amphioxus VCBP* sequence variability (*20*).

may not directly block Dscam-bacteria interactions or may have additional indirect influences on the process of phagocytosis. However, the reduction of phagocytosis is consistent with the loss-of-function in vivo analysis (Fig. 3, B and C) and in vitro binding studies presented below. Taken together, partial but significant reduction in phagocytosis could be achieved by genetic inhibition of expression in hemocytes and by blocking Dscam protein interactions.

We next tested by flow cytometry whether different Dscam isoforms are capable of binding directly to bacteria. Validity of a standard binding assay was tested by using a polyclonal antibody that specifically recognizes *E. coli* epitopes (fig. S6) (*9*), and the same assay was used to test binding of different recombinant Dscam isoforms (Fig. 3, E and F, and fig. S6). All isoforms contained C-terminal Fc tags (*9*), which were used for detection with fluorescently labeled protein A (*9*). Isoforms are designated by the combination of alternative variable Ig domains (*9*). Dscam-1.30.30-Fc and Dscam-7.27.25-Fc contain all of the extracellular domains, whereas Dscam-7.27.13-Fc contains only the N-terminal 9 Ig plus the first FNIII domain. We found that Dscam-7.27.25-Fc and Dscam-7.27.13-Fc could bind to live DH5α *E. coli* bacteria (Fig. 3E and fig. S6). Binding of Dscam-7.27.13-Fc to *E. coli* (Fig. 3E) suggests that the 10 N-terminal domains containing all three variable Ig domains are sufficient for binding. In contrast, binding of isoform Dscam-1.30.30-Fc to *E. coli* is barely detectable (Fig. 3E and fig. S6) and therefore similar to Fc peptides alone or control Ig domains containing antibodies to heavy chain (mouse) (Fig. 3F). It is possible that lack of binding of Dscam-1.30.30-Fc is unique to just this isoform and may not generally reflect the presence of distinct pools of binding and nonbinding isoforms. Therefore, it remains an important task to examine in future studies binding properties of other isoforms. Importantly, the molecular basis of Dscam binding to bacteria is presently unknown, and an assessment of binding specificity will crucially depend on the identification of potentially distinct epitopes on bacteria.

Although we do not know the detailed molecular basis of Dscam function in immune-competent cells, our results are consistent with the possibility that Dscam acts as a signaling receptor or co-receptor during phagocytosis. In addition, binding of Dscam isoforms to bacteria may reflect the possibility that diverse secreted Dscam isoforms are involved in opsonizing invading pathogens in the hemolymph.

Comparative genomic analysis of Dscam-like sequences show high conservation of orthologous *Dscam* genes in Diptera and Hymenoptera orders (*17*). To explore Dscam expression and alternative splicing in other insect orders, we examined Dscam gene structure and expression in the flour beetle *Tribolium castaneum* (Coleoptera) and the silk moth *Bombyx mori* (Lepidoptera) (*18*). Orthologous genes were identified in both species (*9*), and all Dscam-like domains were found to be highly conserved (Fig. 4 and fig. S7). We confirmed the expression of alternative Dscam isoforms by cloning and characterizing 32 cDNAs from *Tribolium* RNA (*Tr-Dscam*) (Fig. 4B) (*9*). Alternatively spliced mRNA segments of *Tr-Dscam* matched corresponding Ig2, Ig3, and Ig7 segments of *Drosophila* Dscam (Fig. 4). RT-PCR and sequencing of Dscam mRNA extracted from fat body tissue of *Tribolium* larvae (*9*) revealed nine different isoform sequences (out of 16 cDNAs) (Fig. 4B). These results suggest that expression of diverse Dscam isoforms in immune-competent fat body cells is conserved among highly diverged insect species.

Our study provides evidence for a potentially extensive repertoire of thousands of Ig-domain-containing proteins in immune-competent cells of insects, which represent an estimated 60% of metazoan species (*19*). Recently, novel and diverse receptor sequences have been identified in jawless vertebrates

(lamprey), protochordates (*Amphioxus*), and mollusks (freshwater snail) (*20*–*22*). It has also been reported that a large class of scavenger receptors (with an estimated 1200 scavenger receptor cysteine-rich domains) are expressed in putative immune effector cells (coelomocytes) of echinoderms (*19*). Similarly, immune responses of crustaceans apparently use an extensive set of diverse antimicrobial peptides (*23*). Although most animals have not acquired adaptive immunity, this apparently broad conservation of receptor diversity strongly suggests important functions, and future studies will have to further address whether the presence of diverse immune receptors in invertebrates increases the effectiveness of immune responses of individual animals. Alternatively, given the relative short life span of many invertebrates, it may be that immune receptor diversity is less important ontogenetically but rather enhances the adaptive potential of animal populations to changing environmental and pathogenic threats.

References and Notes

1. K. Azumi *et al.*, *Immunogenetics* **55**, 570 (2003).
2. L. Du Pasquier, I. Zucchetti, R. De Santis, *Immunol. Rev.* **198**, 233 (2004).
3. D. Schmucker *et al.*, *Cell* **101**, 671 (2000).
4. P. Tzou, E. De Gregorio, B. Lemaitre, *Curr. Opin. Microbiol.* **5**, 102 (2002).
5. *Innate Immunity*, A Ezekowitz, J. Hoffmann, Eds. (Humana, Totowa, NJ, 2003).
6. M. Ramet, P. Manfruelli, A. Pearson, B. Mathey-Prevot, R. A. Ezekowitz, *Nature* **416**, 644 (2002).
7. M. Meister, B. Lemaitre, J. A. Hoffmann, *Bioessays* **19**, 1019 (1997).
8. M. Meister, *Curr. Opin. Immunol.* **16**, 10 (2004).
9. See supporting materials and methods on *Science* Online.
10. C. Samakovlis, D. A. Kimbrell, P. Kylsten, A. Engstrom, D. Hultmark, *EMBO J.* **9**, 2969 (1990).
11. M. Ramet *et al.*, *Immunity* **15**, 1027 (2001).
12. T. Hummel *et al.*, *Neuron* **37**, 221 (2003).
13. X. L. Zhan *et al.*, *Neuron* **43**, 673 (2004).
14. A. Goto *et al.*, *Biochem. J.* **359**, 99 (2001).
15. H. Agaisse, U. M. Petersen, M. Boutros, B. Mathey-Prevot, N. Perrimon, *Dev. Cell* **5**, 441 (2003).
16. A. Holz, B. Bossinger, T. Strasser, W. Janning, R. Klapper, *Development* **130**, 4955 (2003).
17. B. R. Graveley *et al.*, *RNA* **10**, 1499 (2004).
18. *Introduction to Insect Biology and Diversity*, H. V. Daly, J. T. Doyen, A. H. Purcell III, Eds. (Oxford Univ. Press, New York, 1998).
19. Z. Pancer, *Proc. Natl. Acad. Sci. U.S.A.* **97**, 13156 (2000).
20. J. P. Cannon, R. N. Haire, N. Schnitker, M. G. Mueller, G. W. Litman, *Curr. Biol.* **14**, R465 (2004).
21. Z. Pancer *et al.*, *Nature* **430**, 174 (2004).
22. S. M. Zhang, C. M. Adema, T. B. Kepler, E. S. Loker, *Science* **305**, 251 (2004).
23. B. J. Cuthbertson, E. F. Shepard, R. W. Chapman, P. S. Gross, *Immunogenetics* **54**, 442 (2002).
24. G. Neves, J. Zucker, M. Daly, A. Chess, *Nat. Genet.* **36**, 240 (2004).
25. Single-letter abbreviations for the amino acid residues are as follows: A, Ala; C, Cys; D, Asp; E, Glu; F, Phe; G, Gly; H, His; I, Ile; K, Lys; L, Leu; M, Met; N, Asn; P, Pro; Q, Gln; R, Arg; S, Ser; T, Thr; V, Val; W, Trp; and Y, Tyr.

26. We thank S. Sinenko and B. Mathey-Prevot for Hml-GAL4 flies and important advice; H. Agaisse and N. Perrimon for S2 cells, UAS-dslacZ flies, and insightful discussions; S. Brown, Kansas State University, for embryonic RNA from *Tribolium*; and S. Lewis, Tufts University, for *Tribolium* animals; members of Dana-Farber Core Facility and the Mass-Spec Facility at Harvard Medical School (Boston, MA) for the help during LC-MS/MS analysis; W. Wojtowicz, J. Clemens, and L. Zipursky for kindly providing the Dscam-Fc expression constructs; E. Tanner, A. Wakabayashi, and M. Sackal for excellent technical assistance; and C. Weitz, C. Stiles, N. Perrimon, H. Agaisse, B. Mathey-Prevot, J. Green, Q. Ma, and B. Chen for critical reading of the manuscript. This research was supported by a Medical Foundation Award (D.S.), a Pew Scholars Program Award (D.S.), and a John Merck Fund Award (D.S.). Work on the Dscam expression analysis was supported by NIH grant 1RO1-NS46747-01 (D.S.). Sequences have been deposited at GenBank (accession number DQ157471).

Supporting Online Material

www.sciencemag.org/cgi/content/full/1116887/DC1
Materials and Methods
Figs. S1 to S7
Tables S1 and S2
References and Notes

4 July 2005; accepted 8 August 2005
Published online 18 August 2005;
10.1126/science.1116887
Include this information when citing this paper.

Extensive Diversity of Ig-Superfamily Proteins in the Immune System of Insects

Fiona L. Watson *et al.*

Science **309**, 1874 (2005);
DOI: 10.1126/science.1116887

Science (print ISSN 0036-8075; online ISSN 1095-9203) is published weekly, except the last week in December, by the American Association for the Advancement of Science, 1200 New York Avenue NW, Washington, DC 20005.